Original scientific papers UDK 547.56:661.882
doi: 10.7251/COMEN1202153K

NUMERICAL MODELING OF DIFFUSION IN COMPLEX MEDIA WITH SURFACE INTERACTION EFFECTS

M. Kojić[1,2,], M. Milošević[2], N. Kojić[3], M. Ferrari[1], A. Ziemys[1]*

[1] The Methodist Hospital Research Institute, Department of Nanomedicine, 6670 Bertner Ave., R7-116, Houston, TX 77030
[2] Belgrade Metropolitan University - Bioengineering Research and Development Center, BioIRC Kragujevac, Prvoslava Stojanovica 6, 3400 Kragujevac, Serbia
[3] Center for Engineering in Medicine and Surgical Services, Massachusetts General Hospital, Harvard Medical School, Boston, MA 02114

Abstract: Diffusion in natural, technological and biological systems is very common and most important process. Within these systems, which contain complex media, diffusion may depend not only on internal geometry, but also on the chemical interactions between solid phase and transported particles. Modeling remains a challenge due to this complexity. Here we first present a new hierarchical multiscale microstructural model for diffusion within complex media that incorporates both the internal geometry of complex media and the interaction between diffusing particles and surfaces of microstructures. Hierarchical modeling approach, which was introduced in [1], is employed to construct a continuum diffusion model based on a novel numerical homogenization procedure. Using this procedure, we evaluate constitutive material parameters of the continuum model, which include: equivalent bulk diffusion coefficients and the equivalent distances from the solid surface. Here, we examined diffusion of glucose through water using the following two geometrical/material configurations: silica nanofibers, and a complex internal structure consisting of randomly placed nanospheres and nanofibers. This new approach, consisting of microstructural model, numerical homogenization and continuum model, offer a new platform for modeling diffusion within complex media, capable of connecting micro and macro scales.

Keywords: diffusion, hierarchical modeling, complex media, microstructural model, equivalent continuum model, numerical homogenization.

1. INTRODUCTION

In common continuum theories of diffusion through homogenous media Fick's law is used as the fundamental relation:

$$J = -D\nabla c \tag{1}$$

where $\boldsymbol{J}$ is the mass flux along concentration gradient ∇c with diffusion coefficient (diffusivity) D. However, in complex media, phase interface may occupy a substantial portion of diffusion domain so that diffusion transport is affected by molecular interactions with the surface, and predictions following equation (1) may become inaccurate. MD (molecular dynamics) modeling and experiments have shown that diffusive transport of molecules and particles in nanochannels is affected by their proximity to a solid surface [2], [3]. Using MD analysis, it is shown in [2] that molecular diffusivity depends on both concentration and confinement effects. Therefore, modeling of these transport regimes needs novel approaches that could bring molecular scale information into complex macroscale models of nanofluidic devices. An ideal scenario is to properly transfer MD information to macroscopic models. Hierarchical (multiscale) modeling approach, introduced in [1] and which couples MD and Finite Element Method (FEM), offers this possibility.

In this paper we introduce a multiscale hierarchical model for diffusion at the microstructural level (further termed as 'microstuctural model'), within a small reference volume (RV), Figure 3b. The implemented method is effective, robust and generalizable to a variety of problems where diffusion governs transport. Further, we formulate a 'continuum' model which employs the results obtained by the microstructural model for diffusion within the RV. Our method relies on the fundamental condition of the equivalency of mass-release kinetics between the continuum and microstructural models for a given region of space and over a prescribed concentration range. The continuum model is based on constitutive parameters, which include equivalent 'bulk' diffu-

* Corresponding author: mkojic@hsph.harvard.edu

sion coefficients (characterizing free, or Fickian, diffusion within the solvent) and equivalent distances from an imaginary surface (describing surface effects within the microstructure, [1]). Constitutive parameters, depending only on the structural geometry and the material properties of the diffusing constituents, are evaluated for three orthogonal coordinate directions – enabling modeling of general 3D diffusion conditions.

2. METHODS

2.1 MD simulations and scaling function for diffusion coefficient

Molecular Dynamics (MD) has been used for several decades [4]. It is based on statistical mechanics, where motion of particles is described according to the Newtonian mechanics:

$$m_i \dot{\mathbf{v}}_i = \mathbf{F}_i \tag{2}$$

where $m_i, \dot{\mathbf{v}}_i$ and $\mathbf{F}_i$ are mass, acceleration and resulting force (including interaction forces from the neighboring particles and external forces), respectively. The interaction forces include bonded (repulsive-attractive, bending and torsion) and non-bonded (electrostatic, van der Waals) terms. The Force Field (FF) represents a functional form of behavior of chemical structures and is evaluated from potential energy function, $E = E_{intra} + E_{inter}$, of CHARMM FF [5] which is used in our MD models. MD simulations for calculating diffusion coefficients in nanochannels were carried out [1], [6] using NAMD 2.6 [7] with a TIP3P water model [8] and NVT (fixed number of particles N, pressure P, volume V) ensembles. CHARMM compatible amorphous silica force field [9] was employed to model the silica nanochannel, which is modeled by charged hydrophilic amorphous silica phase to match the silica properties after the fabrication process. Glucose diffusion coefficients were calculated from 30 ns trajectories by using the mean square displacement $<r^2>$:

$$<r^2> = 2dDt \tag{3}$$

where the factor d = 1, 2, 3 depends on the dimensionality of the space, and t is time. The diffusivity along the surface normal (z-direction) was evaluated, from the surface up to the middle of the nanochannel. The diffusivity results include dependence on distance from the wall and glucose concentrations (Figure 1 – left panel).

The MD calculated diffusivity is normalized with respect to the "bulk" value D_{bulk} corresponding to diffusivity far from the surface, where influence of the surface is negligible. Hence, we have

$$D = SD_{bulk} \tag{4}$$

where

$$S = S(h, c), \quad 0 \le S \le 1 \tag{5}$$

is the scaling function which depends on the distance from the wall surface h and concentration c. Calculated scaling function is shown in Figure 1 – right panel.

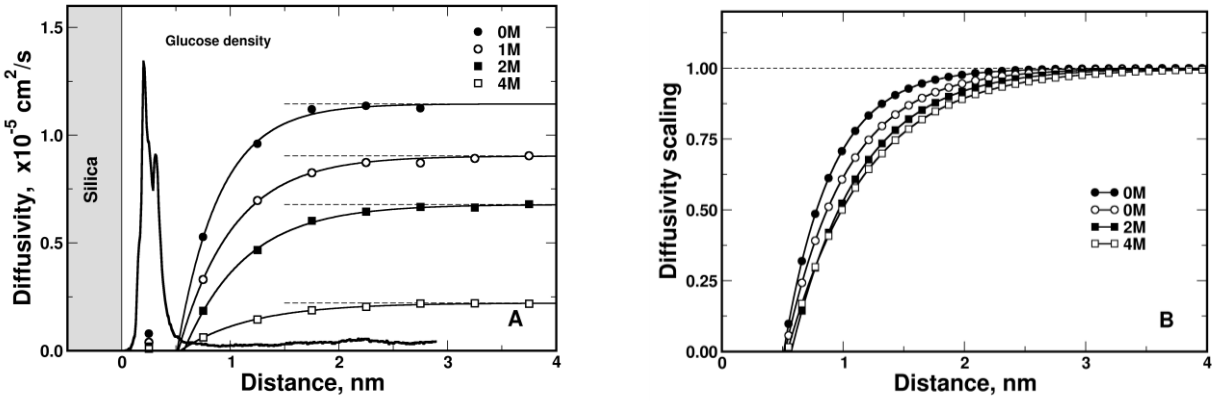

Figure 1. Calculated glucose diffusivity (left panel)) and scaling functions of the proximity to the silica surface for several concentrations (right panel); according to [1].

Experimental investigations showed that $D(\equiv D_{bulk})$ for glucose depends on concentration, although data are quite different (see [1] and references given therein). For examples shown here we

have chosen the glucose D according to the largest data set of [10] that spans over a wide range of concentrations, from 0 to 3.36 M, with linear dependence D(c).

2.2. Finite element model

We here consider unsteady diffusion where the diffusion coefficient depends on both concentration and spatial position of a point within the model. FE solution procedures for nonlinear diffusion problems have been well established and successfully used in various applications (e.g. [11],[12],[13],[14]). The basic mass balance equation, which also includes Fick's law in equation (1), is transformed into the incremental-iterative system of linear balance equations for a finite element [14]:

$$\left(\frac{1}{\Delta t}\mathbf{M}+{}^{n+1}\mathbf{K}^{(i-1)}\right)\Delta\mathbf{C}^{(i)}={}^{n+1}\mathbf{Q}^{S(i-1)}+{}^{n+1}\mathbf{Q}^{V(i)}-{}^{n+1}\mathbf{K}^{(i-1)}\,{}^{n+1}\mathbf{C}^{(i-1)}-\frac{1}{\Delta t}\mathbf{M}\left({}^{n+1}\mathbf{C}^{(i-1)}-{}^{n}\mathbf{C}\right) \tag{6}$$

where **C** is the vector of nodal concentrations; the left upper indices *n* and *n*+1 denote values at the start and end of the time step *n* of size Δt; the indices *i* and *i*-1 correspond to the current and previous equilibrium iteration; $\mathbf{Q}^S$ and $\mathbf{Q}^V$ are surface and volumetric nodal fluxes for the element; and components of the matrices **M** and **K** are

$$M_{IJ}=\int_V N_I N_J dV \tag{7}$$

$${}^{n+1}K_{IJ}^{(i-1)}=\int_V {}^{n+1}D^{(i-1)}N_{I,i}N_{J,i}dV \tag{8}$$

Here N_I and N_J are the interpolation functions, and ${}^{n+1}D^{(i-1)}$ is the diffusion coefficient corresponding to the last known concentration ${}^{n+1}c^{(i-1)}$ at a point within the finite element. Assembly of equations (6) and solution procedures are performed in a usual manner that is well described in the computational mechanics literature (e.g. [11]).

In our models we have incorporated concentration and interface effects, according to equation (4) into the FEM model. Implementation of the expression (4) is illustrated in Figure 2. Note that linear interpolation between scaling curves is used.

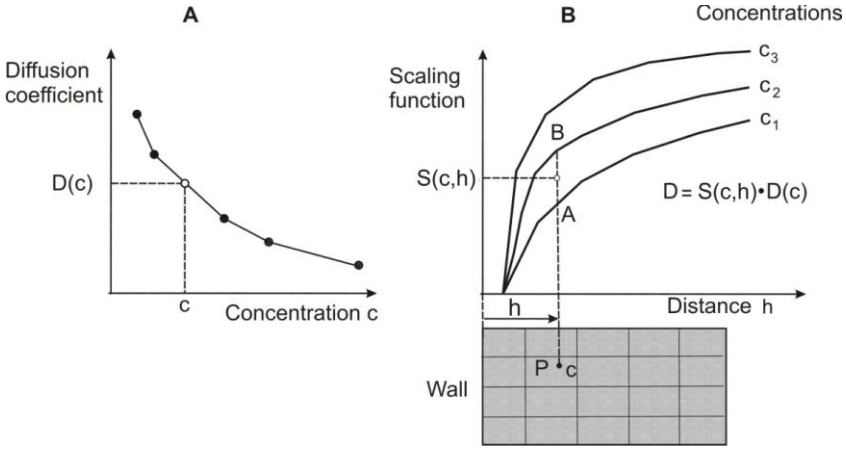

Figure 2. Determination of diffusion coefficient at a spatial point P using dependence on concentration and surface effects. The "bulk" value is first determined from the curve D(c), A; then the scaling function is evaluated from family of curves shown in B. Linear interpolation curves S(c,h) is adopted (between points A and B in the figure); according to [15].

2.3. Generalization of the hierarchical model to porous media

Here we outline a generalization of the hierarchical model to diffusion in complex porous media, consisting of distributed solid constituents within fluid. For simplicity of presentation of this generalization, we assume a medium with solid fibers, as sketched in Figure 3.

The main idea here is to determine equivalent diffusion parameters of a homogenous porous medium which capture the internal structure of a composite medium in a way that diffusion properties are preserved. To achieve this, we first take a reference volume around a material point (in a form of a cube) around that point, Figure 3a, and discretize it into finite elements (Figure 3b). Here we take the real internal microstructure and calculate diffusion in

three orthogonal directions. In this FE model it is possible to properly take into account the surface effects, as sketched in Figure 3c. Namely, for a point A in the medium we calculate distance from the closest fiber surface of an s-group, and evaluate scaling function S_s as described above for diffusion within a nanochannel. We assume that scaling functions are different for the normal and tangential directions, hence we have three scaling functions S^s_ξ, S^s_η, S^s_ς in the local fiber directions ξ,η,ξ, so that the diagonal diffusion matrix (tensor) $D^s_{\xi\xi}, D^s_{\eta\eta}, D^s_{\varsigma\varsigma}$ in the local coordinate system is

$$\begin{aligned} D^s_{\xi\xi} &= S^s_\xi D_{bulk} \\ D^s_{\eta\eta} &= S^s_\eta D_{bulk} \\ D^s_{\varsigma\varsigma} &= S^s_\varsigma D_{bulk} \end{aligned} \qquad (9)$$

where D_{bulk} is the bulk modulus. The diffusion tensor in the global coordinate system *x,y,z* can be obtained by tensorial transformation of the second-order tensor,

$$\mathbf{D}^s_{xyz} = \mathbf{T}^s \mathbf{D}^s_{\xi\eta\varsigma} \mathbf{T}^{sT} \qquad (10)$$

where the components of the transformation matrix contains cosines of angles between local and global axes:

$$T^s_{ij} = \cos(x_i, \xi_j) \qquad i,j=1,2,3 \qquad (11)$$

Here x_i and ξ_j stand for global (*x,y.z*) and local coordinate (ξ,η,ς) systems.

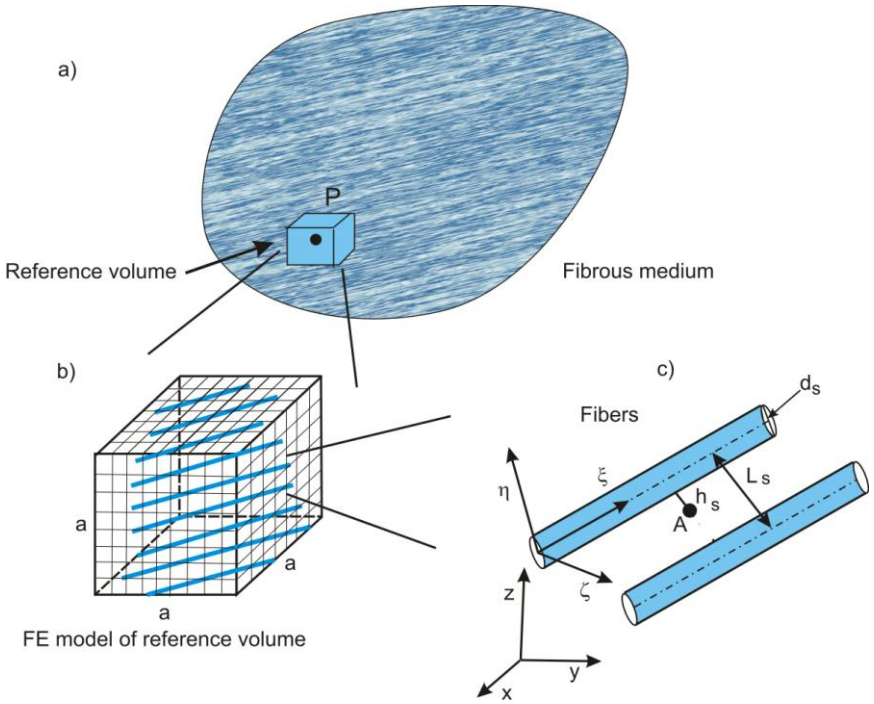

Figure 3. Concept of extension of hierarchical model to porous medium with fibers. a) Fibrous medium with reference volume at a material point P; b) Reference volume discretized into finite elements; c) Geometry of the internal structure – fibers of an s-group, with diameter d_s and with mutual distance L_s, and point A at distance h_s from the fiber surface.

2.4. Numerical homogenization procedure and continuum model

We introduce a novel numerical homogenization procedure to determine the appropriate diffusion properties of a continuum model with a given microstructure. The basic condition governing this procedure is the equivalence of mass fluxes (through any surface in the diffusion domain) for the microstructural and continuum model, at any time during diffusion process. Considering mass release curves for diffusion through an RV around a spatial point, we have that the mass flux J_i in direction x_i is given as

$$J_i = \left(\frac{dm}{dt}\right)_i \qquad (5)$$

This derivative is geometrically represented as the tangent to the mass release curve $m(t)_i$ for the direction x_i, therefore the fluxes are equal for both models if their mass release curves are the same. This interpretation of flux equality through an RV is analogous to the mass balance condition in a differential volume used in continuum mechanics.

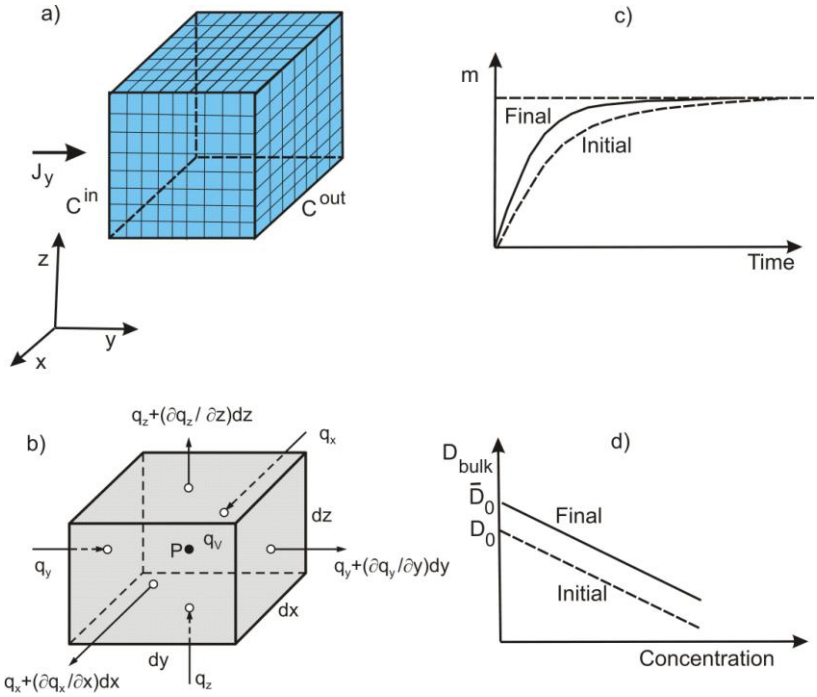

Figure 4. Calculation of diffusion in equivalent homogenous porous medium. a) Reference volume; b) Reference volume in deriving mass balance in differential form (analogy with RV for numerical calculation of equivalent material parameters), q_x, q_y, q_z are surface fluxes, and q_V is volumetric flux; c) Initial and final mass release curve, coinciding with the true mass release curve shown in Figure 4b; d) Assumption about dependence of diffusion coefficient D_{bulk} on concentration – the slope of the line $D_{bulk}(c)$ is the same for the true and equivalent model.

Next, we calculate diffusion through the reference volume using equivalent quantities of a porous homogenous medium within the RV. The porosity *n* is evaluated from the internal structure of the RV. For each diffusion direction *i* (i.e. x,y,z), the steps are as follows:

1. Calculate mass release using initial diffusion using given $D_{bulk}(c)$.

2. Perform changes on the value D_0 until the mass release curve is close enough to the true curve, when the value is $(\bar{D}_0)_i$.

3. Using $(\bar{D}_0)_i$ calculate initial mass release curve taking into account equivalent values of the transformation matrix $\bar{\mathbf{T}}$ and equivalent distance from the solid surface $(\bar{h}_0)_i$.

4. Search for the distance $\bar{h}_i$ when difference between the calculated and true mass release curves is within a selected error tolerance.

In the above calculations of the equivalent transformation matrix and initial equivalent distance $(\bar{h}_0)_i$ a weighted procedure, which takes into account volumes belonging to FE nodes, is implemented (details not given here).

The presented concept of evaluation of parameters related to equivalent homogenous porous medium represents a numerical homogenization procedure. It can be extended to non-homogenous media, by varying equivalent parameters, or to stochastic characteristics. Application of introduced numerical homogenization method (NHM) is illustrated in the Results section.

3. RESULTS

3.1. Effect of fiber direction in RV on mass release results

We are considering diffusion in x direction through RV (Figure 5). RV is a cube with $a = 0.04[\mu m]$, whose entrance surface is connected to a reservoir of volume $V_{in} = 7.850 \cdot 10^{-9}\,\mu l$, with initial concentration $C_{in} = 2.5\ \ mol/l$; while the opposite surface has a constant concentration $C^{out}(=0)$. We investigated examples with two different porosities: 0.951 and 0.558, and with angles of fibers 0, 30, 60 and 90 degrees, with respect to direction of diffusion. Values for fiber's diameter and angles of fiber's direction used in simulations are shown in Table 1. As a result we provided mass release curves, separately for cases of Fickian diffusion and diffusion with surface effects (Figure 6 and 7).

It can be concluded, from results shown in both Fig. 6 and Fig. 7, that deviation from starting mass release curve, which corresponds to the case where direction of fibers is parallel to direction of diffusion, increases with increasing of angle, and is largest when the angle is 90 degrees (diffusion direction is orthogonal to direction of fibers). Additionally, deviations are larger for diffusion with surface effects. It can also be concluded that the deviations are larger for smaller porosities, e.g. with increasing solid phase in the RV.

Table 1. Change of fiber's direction and diameter for two considered porosities of RV.

	0°	30°	60°	90°	Porosity ≈
$D_1(\mu m)$	0.005	0.00482	0.00482	0.005	0.951
$D_3(\mu m)$	0.015	0.0145	0.0145	0.015	0.558

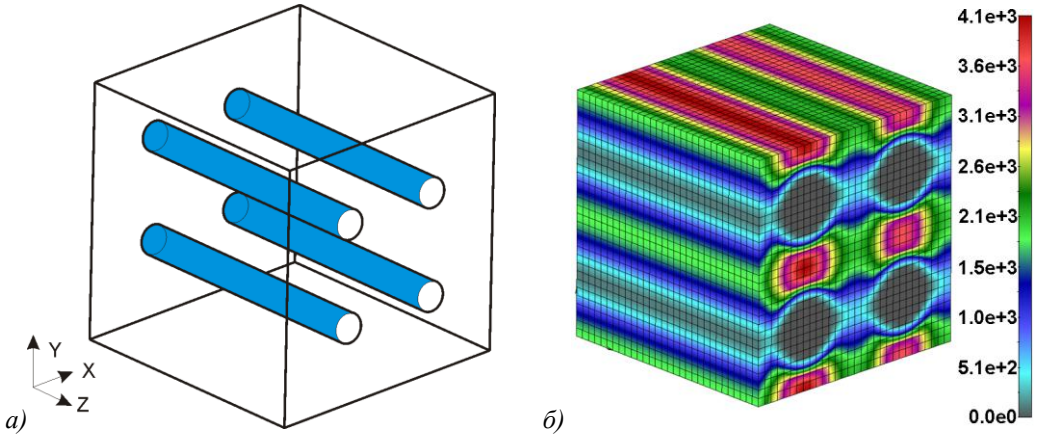

a) *б)*

Figure 5. a) Reference volume with 4 arbitrary placed fibers; b) Field of unit mass flux for first step of simulation, diffusion with surface interaction, RV with 4 fibers whose direction is orthogonal to direction of diffusion.

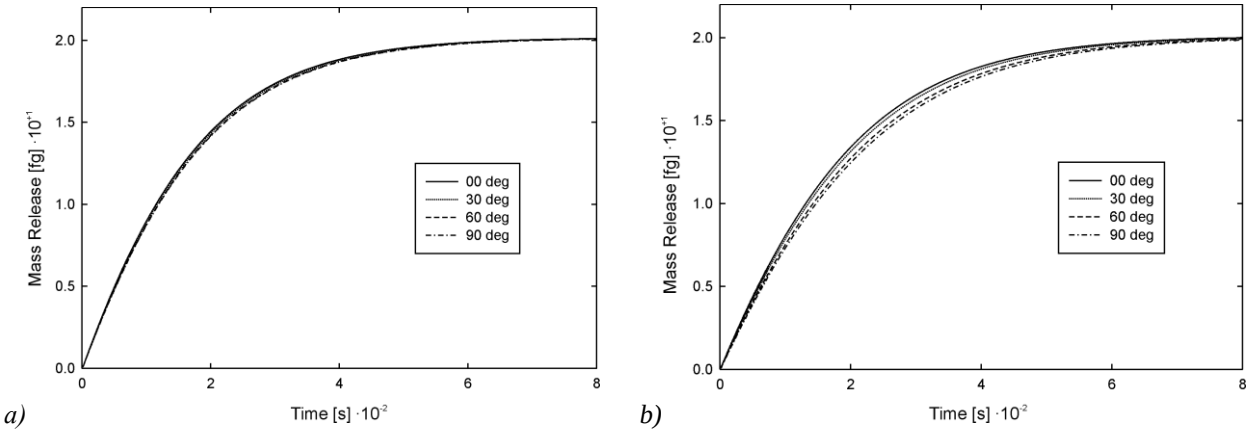

a) *b)*

Figure 6. Mass release curves for different direction of fibers, porosity = 0.951: a) Fickian diffusion; b) Diffusion with surface interaction effects.

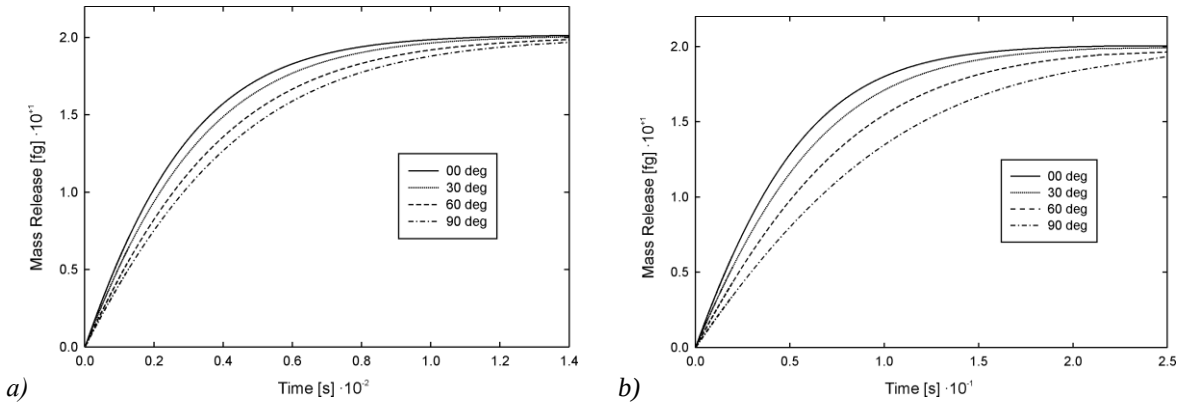

Figure 7. Mass release curves for different direction of fibers, porosity = 0. 558: a) Fickian diffusion; b) Diffusion with surface interaction effects.

3.2. Dependence of equivalent parameters on concentration range and concentration gradient

For given solvent and diffusing particles we show that material parameters of the continuum model (equivalent diffusion coefficients and equivalent distances from surface) depend only on the geometry of the microstructure and its material characteristics [16]. To demonstrate this statement, we take a reference volume (RV) with solid silica nanofibers (as shown in Figure 5), with fibers diameters of 10nm, angle of fiber direction of 75 degrees (with respect to diffusion direction) and porosity of 80%. For this model we change the boundary conditions to achieve various mass release curves.

In Figure 8a are shown three mass release curves which differ significantly, obtained by changing inlet reservoir volume V_{in} for one order of magnitude (from 1.57×10^{-9} to 7.85×10^{-8} [μl]). Equivalent diffusion coefficient $\bar{D}$ and equivalent distance $\bar{h}$ are given in Table 2; they are practically the same for all mass release curves.

Another way to change mass release curves is to change initial concentration c_0 . We have changed c_0 from 0.01 to 2.75 *Molar*, while keeping V_{in} unchanged. Mass release curves are shown in Figure 8b, while the calculated $\bar{D}$ and $\bar{h}$ are given in Table 3. Again, we see that equivalent diffusion coefficient $\bar{D}$ and distance from surface $\bar{h}$ remain essentially unchanged.

Table 2. Material parameters $\bar{D}_x$ u $\bar{h}_x$ for four reservoir volumes V_{in}, (initial concentration $c_0 = 2.75$ mol / l).

No.	V_{in} $[\mu l]$	$\bar{D}_x$ $[\mu m^2 / hour]$	$\bar{h}_x$ $[\mu m]$
1	$7.850\cdot10^{-8}$	$5.4864\cdot10^{+7}$	$2.2373\cdot10^{-3}$
2	$1.570\cdot10^{-8}$	$5.4864\cdot10^{+7}$	$2.2373\cdot10^{-3}$
3	$7.850\cdot10^{-9}$	$5.4864\cdot10^{+7}$	$2.2373\cdot10^{-3}$
4	$1.570\cdot10^{-9}$	$5.4864\cdot10^{+7}$	$2.2373\cdot10^{-3}$

Table 3. Material parameters $\bar{D}_x$ and $\bar{h}_x$ for three initial inlet concentrations c_0 (with constant $V_{in} = 7.850\cdot10^{-9}\,\mu l$).

No.	C_{in} $[mol / l]$	$\bar{D}_x$ $[\mu m^2 / hour]$	$\bar{h}_x$ $[\mu m]$
1	2.75	$5.4864\cdot10^{+7}$	$2.2373\cdot10^{-3}$
2	1.75	$5.4864\cdot10^{+7}$	$2.1971\cdot10^{-3}$
3	0.01	$5.4864\cdot10^{+7}$	$2.0765\cdot10^{-3}$

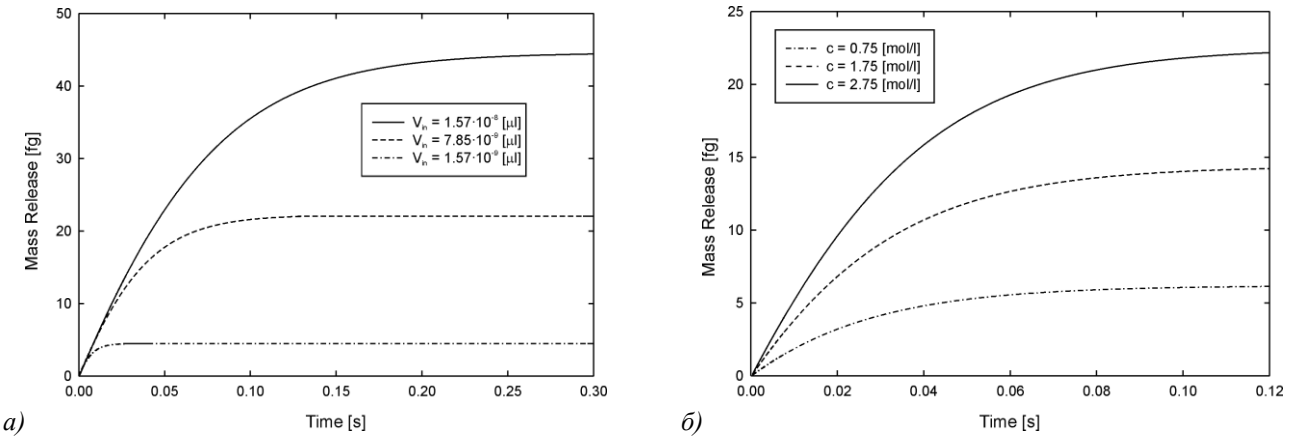

Figure 8. a) Mass release curves for volumes of inlet reservoir from Table 2. (μl): $1.570\cdot10^{-8}$, $7.850\cdot10^{-9}$ u $1.570\cdot10^{-9}$; b) Mass release curves obtained for inlet reservoir volume $V_{in}=7.850\cdot10^{-9}\,\mu l$, and four initial concentrations of the inlet reservoir c_0 (Molar): 2.75, 1.75, 0.75 u 0.01.

3.3. Dependence of equivalent parameters on dimension of RV

In this example we have doubled dimensions of the RV and calculated $\bar{D}$ and $\bar{h}$. Geometry of two RVs used in this example is shown in Figures 9a and 9b. For those two models we used the following data:

1. Model 1: cube side $a_1=0.04[\mu m]$, volume of RV: $V^1=7.850\cdot10^{-9}\,\mu l$, number of fibers in RV is N_1 =2*2 = 4, length of fibers is $l_1=0.04[\mu m]$.

2. Model 2: cube side $a_2=2a_1=0.08[\mu m]$, volume of RV: $V^2=8V^1$, number of fibers in RV $N_2=4N_1$ =4*4 = 16, length of fibers is $l_2=0.08[\mu m]$.

Tables 4 and 5 demonstrate that these material parameters are independent of the RV size. We obtained similar results for an RV consisting of spheres, but those results are not given here (given in [16]).

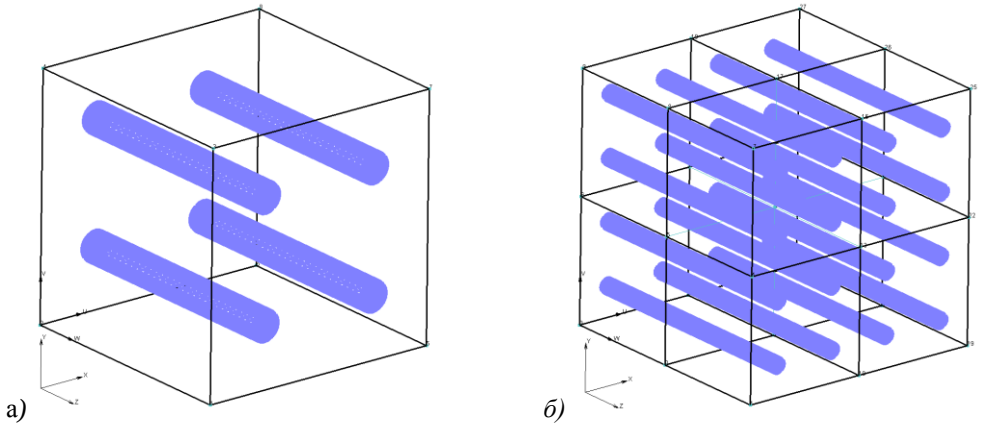

Figure 9. RV of two models used for investigating dependence of equivalent parameters on dimension of RV: a) Geometry of model 1; b) Geometry of model 2.

Table 4. Material parameters $\bar{D}_x$ and $\bar{h}_x$ for two sizes of the RV (for $c_0=2.75$ Mol / l , $V_{in}=7.850\cdot10^{-9}\,\mu l$)

No.	$a\ [\mu m]$	$\bar{D}_x\ [\mu m^2/hour]$	$\bar{h}_x\ [\mu m]$
1	0.04	$5.5128\cdot10^{+7}$	$2.1615\cdot10^{-3}$
2	0.08	$5.4864\cdot10^{+7}$	$2.1827\cdot10^{-3}$

Table 5. Material parameters $\bar{D}_x$ *u* $\bar{h}_x$ *for two sizes of the RV (for* $c_0 = 0.01$ *Mol / l ,* $V_{in} = 7.850 \cdot 10^{-9}$ *μl)*

No.	a $[\mu m]$	$\bar{D}_x$ $[\mu m^2 / hour]$	$\bar{h}_x$ $[\mu m]$
1	0.04	$5.4864 \cdot 10^{+7}$	$2.0730 \cdot 10^{-3}$
2	0.08	$5.4864 \cdot 10^{+7}$	$2.0450 \cdot 10^{-3}$

3.4. Effect of the total fiber's area in RV on values of equivalent parameters

Here we present the effects of total fiber's area in RV on equivalent parameters of continuum model. We consider RV with the same dimensions and input parameters as in the previous examples. The cube side is $a = 0.04 \mu m$, inlet reservoir is with $V_{in} = 7.850 \cdot 10^{-9} \mu l$ volume and with initial concentration $C_{in} = 2.75$ mol / l; while the inlet reservoir is with infinitely large volume. Diffusion coefficient is changing linearly from $D_0 = 5.9616 \cdot 10^7$ [μm^2/*hour*] for C=0, to $D_1 = 1.9006 \cdot 10^7$ [μm^2/*hour*] for C=2.75 [*molar*]. In order to check the influence of total fibers' surface area we used tree different configurations of internal microstructure, consisting of fibers whose direction is orthogonal to direction of diffusion. All examples are approximately with 80% porosity. Input parameter for each example, together with the calculated values of total surface areas and total volume of solid phase in the system, are given in Table 6.

Table 6. Input parameters for three examples of internal microstructures, together with calculated values of total surface area and total volume of solid phase in RV.

	D_{fib} μm	Fiber's mesh	P_{fib} μm^2	V_{fib} μm^3	Porosity
Example 1	0.00500	4x4	0.010050	1.2566e-5	0.803891
Example 2	0.00675	3x3	0.007634	1.2566e-5	0.800347
Example 3	0.01000	2x2	0.005026	1.2566e-5	0.805556

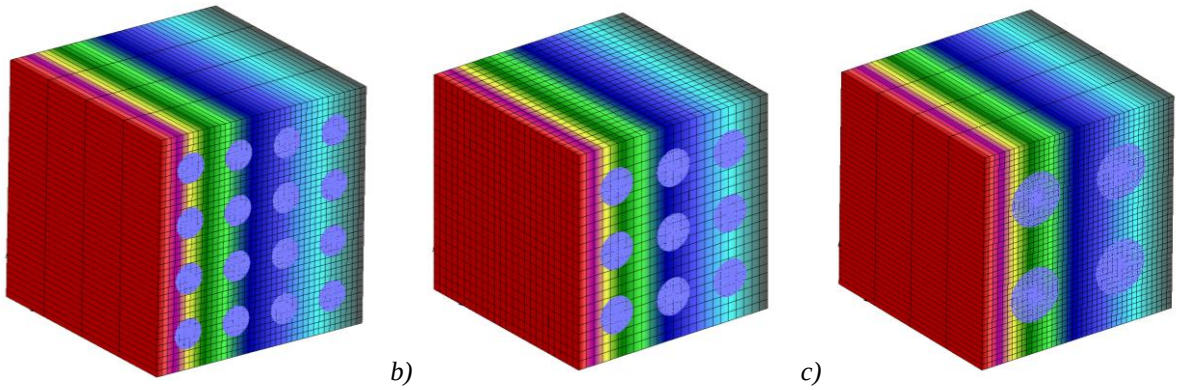

a) *b)* *c)*

Figure 10. RV with fibers orthogonal to direction of diffusion. Field of concentration for continuum model and for first time step of simulation. a) Example 1, 16 fibers with 5 nm diameter; b) Example 2, 9 fibers with 6.75 nm diameter; c) Example 3, 4 fibers with 10 nm diameter.

Results for equivalent diffusion coefficient of free diffusion and equivalent distance from the surface for diffusion in *x* direction, calculated using numerical procedure of homogenization are shown in Table 7. According to results for $\bar{D}_0^{eff}$ from table 7 it can be concluded that equivalent diffusion coefficient of free diffusion depends on porosity (results for $\bar{D}_0^{eff}$ are approximately the same for all three examples). Results for equivalent distance from the surface H_{eff} show that H_{eff} depends on the total surface area in the system (H_{eff} decreases with increasing of total surface area). Decreasing of H_{eff} leads to the slower kinetics of diffusion process which is one of the proofs showing that that the surface interaction in nanoconfined space substantially affects diffusion process.

Table 7. Equivalent diffusion coefficient of free diffusion and equivalent distance from the surface for diffusion in X direction, calculated using numerical homogenization procedures for examples from Figure 6.4.7.

	$\bar{D}_0^{eff}$	$\bar{D}_1^{eff}$	Surface Area [μm^2]	H_{eff}
Example 1	4.33908e+7	2.78251e+6	0.010050	1.6768E-3
Example 2	4.33800e+7	2.77214e+6	0.007634	1.9002E-3
Example 3	4.34844e+7	2.87622e+6	0.005026	2.2727E-3

3.6. Validation of microstructure model

We have calculated diffusion in a porous material, with a nanospheres geometry using our microstructural model. This corresponds to the diffusion conditions described in [17]. Calculation was performed by neglecting surface effects (Fickian diffusion) and for various porosities, using an RV. Our curve for the ratio of the effective diffusion coefficient $\bar{D}$ to the bulk value D_0, $\bar{D}/D_0$, shows very good agreement with values obtained by analytical homogenization procedure in [17]. Dependence $\bar{D}/D_0$ on porosity ϕ was earlier obtained according to a self-consistent analytical method [18], and can be expressed in a simple form:

$$\bar{D}/D_0 = \frac{2\phi}{3-\phi} \tag{6}$$

Results of this simple formula are displayed by dashed line in Fig. 11; deviation from our solution and [17] becomes apparent for smaller porosities.

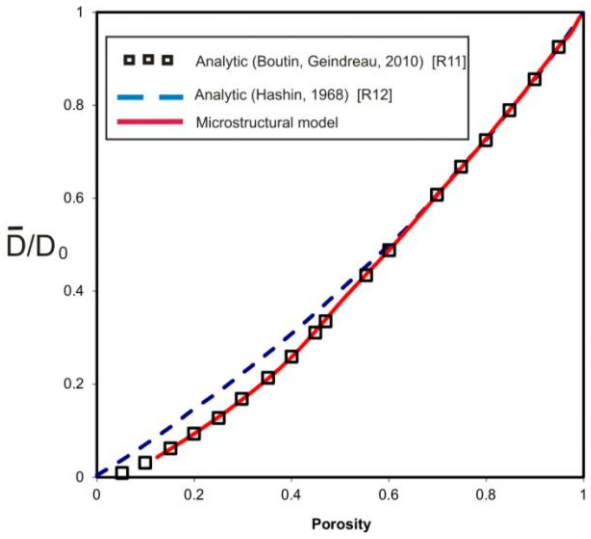

Figure 11. Ratio of the effective diffusion coefficient $\bar{D}$ with respect to the bulk value D_0, in terms of porosity. Our microstructural structure consists of spheres. Surface interaction is neglected, hence Fickian diffusion is assumed. Two analytical solutions are shown, according to [17],[18].

3.7. Diffusion through reference volume with spheres

In RV with cubic shape (cube side is $a = 0.04\mu m$), we uniformly placed 27 silicon spheres (Figure 12). Diameter of sphere is $D_s = 0.009\mu m$, sphere network is 3x3x3, and porosity of internal microstructure is 89.8%. Volume of inlet reservoir is $V_{in} = 7.85 \cdot 10^{-9}\mu l$ and concentration is 2.75 *molar*, while outlet reservoir is with infinitely large volume.

Field of concentration and unit mass flux at first step (t=0.004s) of simulation for diffusion with surface effects are shown on Fig. 13a and Fig. 14a, while the same field in planes X-Y at distance Z=0.02 μm are shown on Fig. 13b and Fig. 14b.

For the example shown in Figure 12 we performed numerical homogenization procedure, both for Fickian diffusion and diffusion with surface effects.

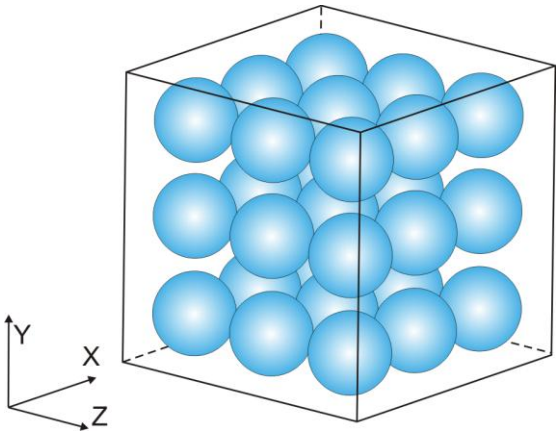

Figure 12. Internal microstructure of reference volume, consisting of 27 spheres, porosity is 89.8%.

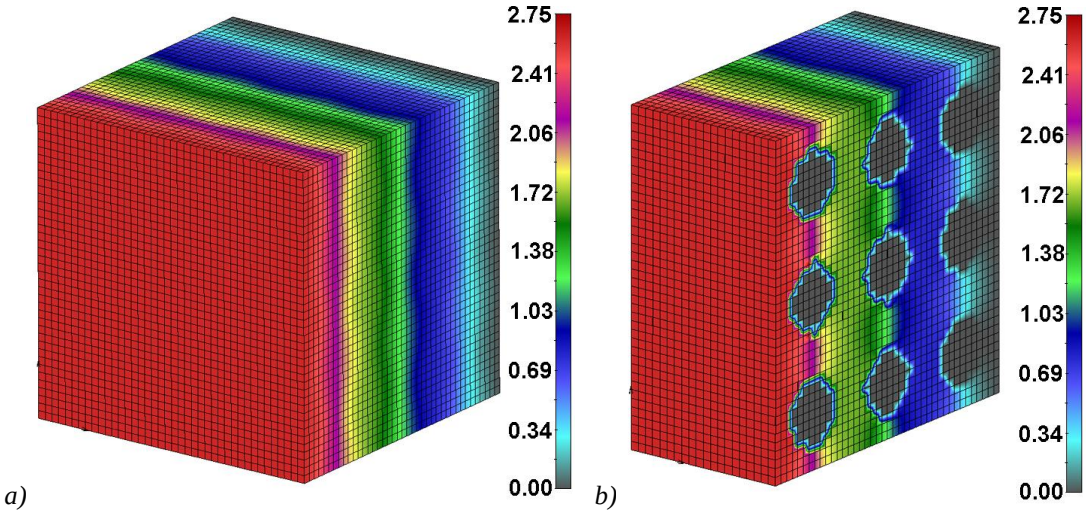

Figure 13. Field of concentration, diffusion in X direction, microstructural model with spheres, a) first step of simulation, t= 0.004s; b) plane X-Y at distance Z=0.02 μm .

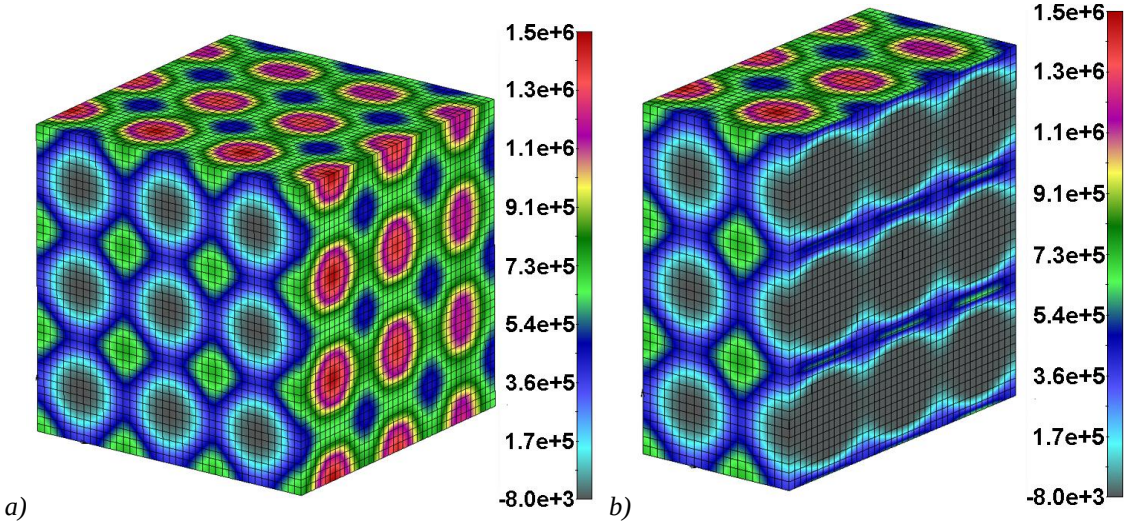

Figure 14. Field of unit mass flux, diffusion in x direction, microstructural model with spheres: a) first step of simulation, t= 0.004s; b) plane X-Y at distance Z=0.02 μm .

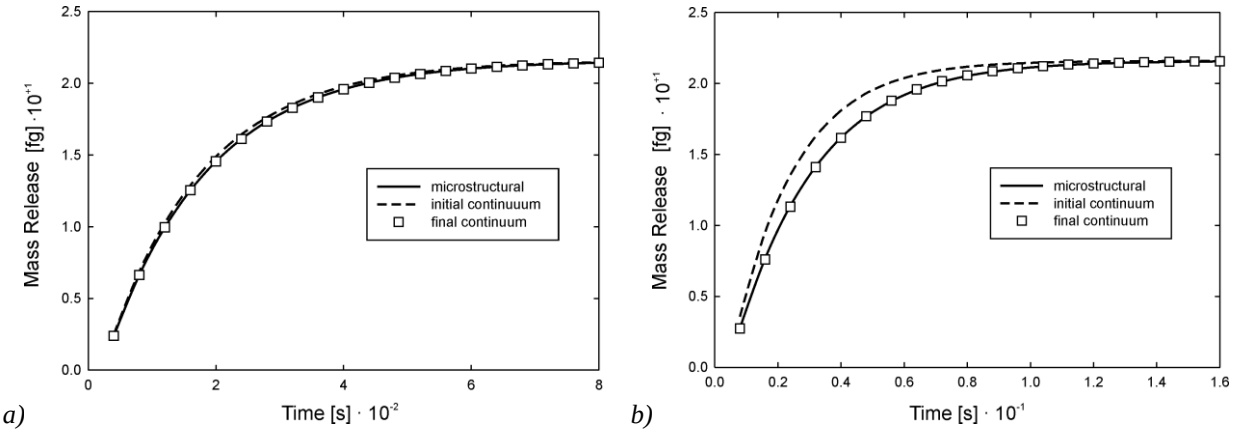

Figure 15. Mass release curves for internal microstructure shown in Figure 12. a) Curves for microstructural model with D(c), continuum model with estimated D(c), and continuum model with final D(c); b) Curves for microstructural model with D(h,c), continuum model with estimated D(h,c), and continuum model with final D(h,c).

Mass release curves for Fickian and diffusion with surface effects, for either microstructural, initial and final continuum models, are displayed in Fig. 15a and Fig. 15b.

4. SUMMARY AND CONCLUSIONS

In summary, we have first formulated a microstructural hierarchical diffusion model, which includes surface interaction effects, for a general microstructural geometry. In this model, the interaction effects are incorporated through scaling functions (evaluated using MD), which represent the ratios between the real and bulk diffusion coefficients. The scaling functions, expressed in terms of distance from the solid surfaces and concentration, are calculated in the local coordinate system of the solid surface. Therefore, two domains of diffusion are distinguished: the bulk diffusion domain (with Fickian diffusion) and the domain near surfaces, with non-Fickian hindered diffusion. In both domains, diffusion is calculated by using the FE method. The surface effects become apparent when comparing the slower mass release kinetics (with surface interactions) with purely Fickian mass release (without surface effects).

This microstructural model is then employed within a novel numerical homogenization procedure to establish the equivalent continuum diffusion model. The procedure is general since it is applicable to an internal, structural geometry of any complexity, and can include different solid material sets with different material properties. The procedure relies on the condition that mass release curves of the two models must be equal. Constitutive diffusion parameters of the continuum model are determined for the three coordinate directions and include the traditional bulk diffusion coefficients, and also equivalent distances from the solid surfaces to account for surface interaction effects on diffusion. Furthermore, these constitutive parameters can depend on the local concentration.

Numerical homogenization procedure presented in this work is analogous to homogenization procedures previously presented in linear and nonlinear solid mechanics, heat transfer and diffusion, where different types of RV were used (e.g. [19],[20],[21]). Previous homogenization procedures have limitations due to the special assumptions made regarding microstructure (e.g. periodicity) as well as relying on various asymptotic expansions of analytic forms. Our method is not only general, but also includes concentration-dependent parameters within a wide range of concentrations over which diffusion occurs.

5. ACKNOWLEDGMENTS

This project has been supported with federal funds from NASA under the contracts NNJ06HE06A and NNX08AW91G, Department of Defense under the contract DODW81XWH-09-1-0212, as well as funds from State of Texas Emerging Technology Fund, Nano Medical Systems (NMS), Alliance of NanoHealth (ANH), and University of Texas at Houston. The authors acknowledge the Texas Advanced Computing Center (TACC) at The University of Texas at Austin for providing HPC resources that have contributed to the research results reported within this paper.

The authors acknowledge support from Ministry of Education and Science of Serbia, grants OI

174028 and III 41007, City of Kragujevac, and from FP7-ICT-2007 project (grant agreement 224297, ARTreat).

6. REFERENCES

[1] A. Ziemys, M. Kojić, M. Milošević, N. Kojić, F. Hussain, M. Ferrari, A. Grattoni, *Hierarchical modeling of diffusive transport through nanochannels by coupling molecular dynamics with finite element method*, Journal of Computational Physics, Vol. 230 (2011) 5722–5731.

[2] A. Ziemys, A. Grattoni, D. Fine, F. Hussain, M. Ferrari, *Confinement effects on monosaccharide transport in nanochannels*, The Journal of Physical Chemistry B 114−34 (2010) 1117−11126.

[3] N. Aggarwal, J. Sood, K. Tankeshwar, *Anisotropic diffusion of a fluid confined to different geometries at the nanoscale.* Nanotechnology, Vol. 18−33 (2007) 5.

[4] D. C. Rapaport, *The Art of Molecular Dynamics Simulation*, Cambridge University Press, (2004).

[5] A. Jr MacKerell, et al., *CHARMM: The Energy Function and Its Parameterization with an Overview of the Program*, J. Phys. Chem. B, Vol. 102−18 (1998) 3586-3616

[6] A. Ziemys, M. Ferrari, C. N. Cavasotto, *Molecular Modeling of Glucose Diffusivity in Silica Nanochannels*. J. Nanosci. Nanotechnol., Vol. 9 (2009) 6349–6359.

[7] J. C. Phillips, R. Braun, W. Wang, J. Gumbart, E. Tajkhorshid, E. Villa, C. Chipot, R. D. Skeel, L. Kale´, K. Schulten, *Scalable molecular dynamics with NAMD*. J. Comput. Chem., Vol. 26 (2005) 1781–1802.

[8] W. L. Jorgensen, J. Chandrasekhar, J. D. Madura, R. W. Impey, M. L. Klein, *Comparison of simple potential functions for simulating liquid water*. J. Chem. Phys., Vol. 79 (1983) 926–935.

[9] E. R. Cruz-Chu, A. Aksimentiev, K. Schulten, *Water-silica force field for simulating nanodevices*. J. Phys. Chem. B, Vol. 110 (2006) 21497–21508.

[10] J. K. Gladden, M. Dole, *Diffusion in supersaturated solution-II: glucose solutions.* J. Am. Chem. Soc., Vol. 75 (1953) 3900−3904.

[11] K. J. Bathe, *Finite Element Procedures*. Prentice-Hall, Inc., Englewood Cliffs, N.J., 1996.

[12] T. Hughes, *The finite element method: linear static and dynamic finite element analysis*. 2000, New York: Dover Publications.

[13] N. Kojic, A. Kojic, and M. Kojic, *Numerical determination of the solvent diffusion coefficient in a concentrated polymer solution.* Communications in Numerical Methods in Engineering, Vol. 22−9 (2006) 1003−1013.

[14] M. Kojic, N. Filipovic, B. Stojanovic, and N.Kojic, *Computer Modeling in Bioengineering*, Theoretical Background, Examples and Software, J Wiley and Sons, Chichester, 2008.

[15] M. Kojić, M. Milošević, N. Kojić, M. Ferrari, A. Ziemys, *On diffusion in nanospace*, JSSCM, Vol. 5−1 (2011) 84−109.

[16] M. Kojić, M. Milošević, N. Kojić, M. Ferrari, A. Ziemus, *Diffusion in composite materials with surface interaction effects: microstructural and continuum models*, Nature Materials (to be submitted), 2012.

[17] C. Boutin, C. Geindreau, *Periodic homogenization and consistent estimates of transport parameters through sphere and polyhedron packings in the whole porosity range*, Phys. Rev. E, Vol. 82 (2010) 036313.

[18] Z. Hashin, *Assessment of the self-consistent scheme approximation*, J. Compos. Mater., Vol. 2 (1968) 284.

[19] M. O. Nicolas, J. T. Oden, K. Vemagantia and J. F. Remacle, *Simplified methods and a posteriori estimation for the homogenization of representative volume elements*, Comput. Methods Appl. Mech. Engrg., Vol. 176 (1999) 265−278

[20] S. J. Chapman, R. J. Shipley, R. Jawad, *Multiscale modelling of fluid flow in tumours*, Bull. Math. Biology, Vol. 70 (2008) 2334–2357

[21] W. Yu, T. Tnag, *Variational asymptotic method for unit cell homogenization of periodically heterogeneous materials*, Int. J. Solids Struct., Vol. 44 (22−23), (2007) 7510–7525.

ꕥ

НУМЕРИЧКО МОДЕЛИРАЊЕ ДИФУЗИЈЕ У КОМПОЗИТНОМ МЕДИЈУМУ СА УКЉУЧЕНИМ УТИЦАЈЕМ ПОВРШИНА

Сажетак: Дифузија представља један од најбитнијих процеса у природним, технолошким и биолошким системима. У оквиру ових система, који су облика сложеног медијума, на дифузију не утиче само унутрашња геометрија микро-

структуре система, већ и хемијска интеракција између молекула који се крећу и површина солида у систему. Стога, моделирање транспорта материје кроз ове сложене медијуме представља велики изазов за научнике данашњег времена. У овом раду ћемо прво представити генерализацију хијерархијског модела повезивањем више скала, који укључује утицај унутрашње геометрије комплексног медијума и међусобну интеракцију између молекула и површина солида, на микроструктурне моделе дифузије у комплексним медијумима. На основу принципа хијерархијског модела, који је први пут представљен у [1], помоћу процедуре нумеричке хомогенизације врши се генерисање континуум дифузионог модела. Коришћењем хомогенизације се затим одређују конститутивни материјални параметри континуум модела, у које спадају: еквивалентни дифузиони коефицијенти слободне дифузије и еквивалентна растојања од површине солида. На крају рада ће бити приказани примери дифузије молекула глукозе кроз водени раствор коришћењем две различите конфигурације: домен са силиконским нановлакнима као и домен са сложеном унутрашњом микроструктуром која се састоји из произвољно распоређених нановлакана и наносфера. Овде описани приступ, који се састоји из микро-структурног модела, нумеричке хомогенизације и континуум модела, представља нов начин моделирања дифузије у сложеним медијумима, способан да повеже процесе који се посматрају на микро и макроскали**.**

Кључне речи: дифузија, хијерархијски модел, сложени медијум, микроструктурни модел, еквивалентни континуум модел, нумеричка хомогенизација.